

Use Of Autonomous Profiling Floats For Validation And Calibration Of Satellite Ocean Color Estimates

Gregory Gerbi, Skidmore College, Saratoga Springs, NY, United States

Emmanuel Boss, University of Maine, Orono, ME, United States

Robert Fleming, University of Maine, Orono, ME, United States

David Antoine, Laboratoire d'Océanographie de Villefranche, Villefranche-sur-Mer, France

Keith Brown, Satlantic, Halifax, Nova Scotia, Canada

Andrew Barnard, WETLabs, Philomath, Oregon, United States

Matthew DeDonato, Teledyne Webb Research, East Falmouth, Massachusetts, United States

William Woodward, CLS America, Lanham, Maryland, United States

Chris Proctor, NASA GSFC Ocean Biology Processing Group, Greenbelt, MD, United States

1. INTRODUCTION

In order to accurately calibrate satellite-based measurements of ocean color, *in situ* measurements of radiometric quantities are necessary (see Hooker et al. (2007)). Traditionally, these measurements have been made at fixed moorings, BOUSSOLE, in the Mediterranean Sea (Antoine et al. 2008), and MOBY, near Hawaii (Clark et al. 2003). Recent work has shown that shipboard measurements may produce *in situ* measurements of quality as high as those made at MOBY (Bailey et al. 2008; Voss et al. 2010). In addition, an indirect method using spectra modeled from chlorophyll-a concentrations has also been shown to agree well with buoy-based calibration of data from SeaWiFS (Werdell et al. 2007).

This document presents preliminary results of the development and use of autonomous profiling floats to make *in situ* measurements for calibration and validation of ocean color satellite observations. Significant hardware and software integration was performed to develop the floats described here and to make the system commercially available. We describe the system and techniques of measurement and estimation, and we show comparisons of the float observations to both mooring (MOBY and BOUSSOLE) and satellite measurements (MODIS Aqua and VIIRS).

2. METHODS

a. Platform

The observations described here are made from an autonomous profiling float with integrated optical instruments. The float is an Apex float built by Teledyne Webb Research and similar to many of those used in the Argo program (<http://www.argo.ucsd.edu/>). Sampling is controlled through a configuration file that can be changed after each profile via two-way satellite communication. The flexible sampling capabilities of the float allow for both burst and continuous sampling.

Instruments on the float (figure 1) are a Seabird SBE 41CP CTD with a Druck pressure sensor, Aanderra Oxygen Optode, WET Labs BB2FL with backscatter at 412 and 440 nm and dissolved organic matter fluorescence, WET Labs FLBB with backscatter at 700 nm and chlorophyll fluorescence, WET Labs C-Rover 7 beam transmissometer (650 nm), Satlantic OCR 504 radiometers with upwelling radiance and downwelling irradiance sensors at 412, 443, 490, and 555 nm. The Optode

is integrated into the float and the optical instruments are combined into what is now a commercially available product (<http://satlantic.com/boss>).

Because Apex floats were not originally designed for detailed near-surface measurements, many modifications to float behavior were needed, and a few challenges remain. Most of these relate to buoyancy control and pressure measurements. The float is slow buoyancy adjustments are made based on estimates of ascent rate, so they adjust somewhat slowly as the ambient buoyancy changes. Thus, the

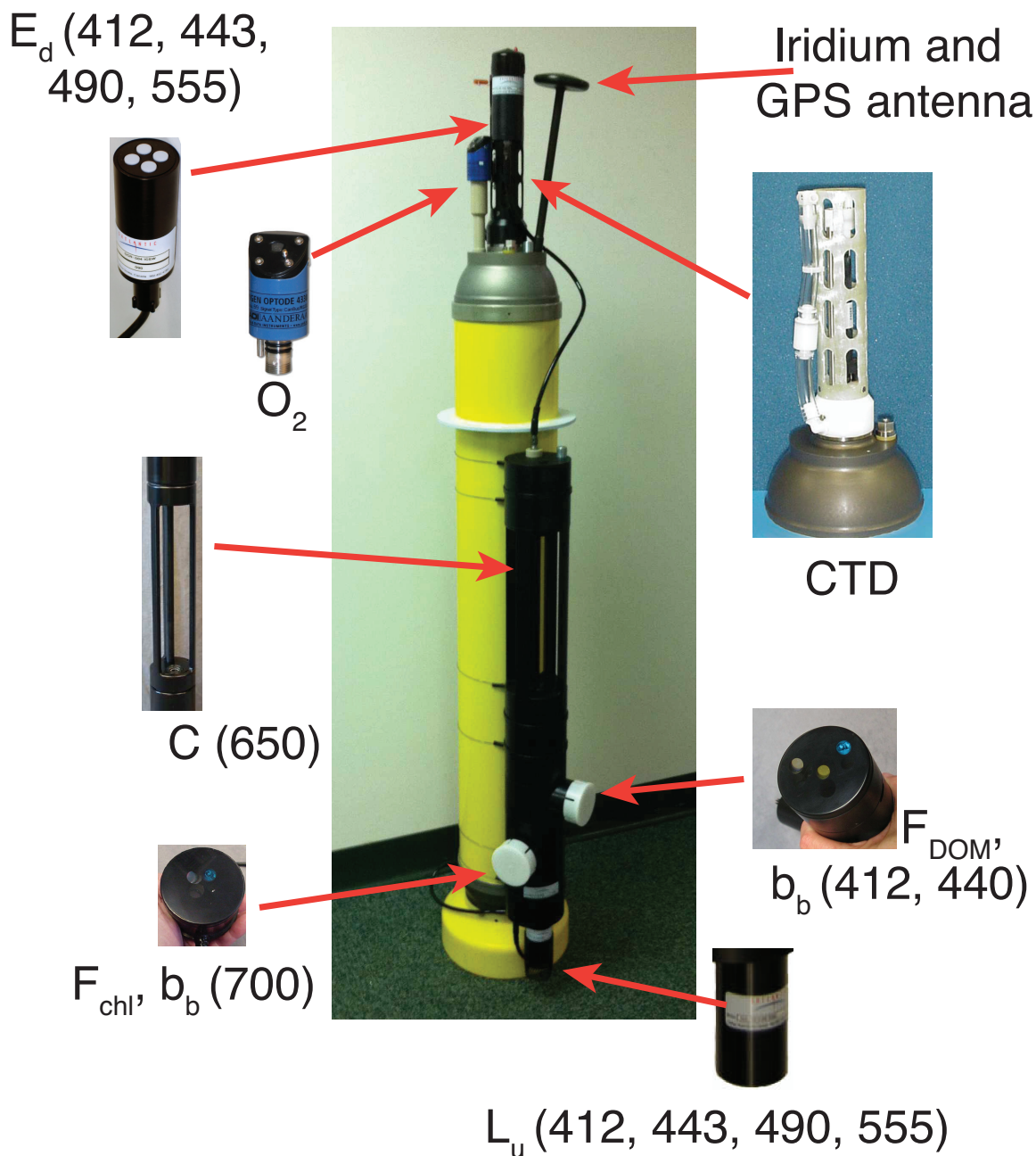


FIG. 1. Picture of biogeochemical float, with representative details of individual instruments.

ascent rate of the float in water of rapidly changing density is not constant (figure 2). Because of this, and the need for accurate pressure measurements near the sea surface, an additional feature was developed that allowed rapid sampling (every 2-3 seconds) of the pressure sensor near the sea surface.

b. Deployments

Results presented here are from three deployments. Each deployment had two floats. One was in summer, 2011, near BOUSSOLE in the Mediterranean, one was in December, 2011, near MOBY in Hawaii, and one was in May, 2012, in the north Atlantic northwest of Bermuda. During the Hawaii deployment one of the downwelling irradiance radiometers was damaged, so while we have L_u measurements from both floats we have remote sensing reflectance measurements from only one.

The Mediterranean deployments were both short, with 29 profiles from each float. Floats from the Hawaiian deployment are still operational, with each having made more than 150 profiles. The north Atlantic deployment is also still ongoing, with each float having made 88 profiles. In this study we ended our analysis period in mid August, examining about 15 fewer profiles than just mentioned for each of the active floats.

c. Estimating remote sensing reflectance

The goal of this study is to develop a method of using autonomous floats for calibration and validation of satellite ocean color measurements. For the majority of the deployments the floats have profiled every two days. Each profile begins with the float parking at 1000 m depth for about one and a half days. This depth is chosen to minimize the biofouling that would occur closer to the surface. The ascent to the surface takes several hours with an ascent rate at depth of about 8 cm/s and ascent rate near the surface of about 4 cm/s. This study uses burst sampling at depths deeper than 20 m. At shallower depths the the optical instruments are sampled continuously at 1 Hz. After the profile the float remains at the sea surface for five minutes. A single time averaged estimate of L_u and E_d is made during the surface interval. Self-shading of the radiance upwelling sensor has not yet been addressed in our estimates of L_u .

Estimating remote sensing reflectance requires estimates of upwelling radiance and downwelling irradiance above the air-water interface. The irradiance sensor is out of the water during the surface interval, but the radiance sensor is more than a meter below the surface. We extrapolate L_u to the surface using an integrated form of Gershun's equation in one dimension

$$L_u(z) = L_u(z_0)e^{K_d(z-z_0)}, \quad (1)$$

where K_d is the diffuse attenuation coefficient, z is the vertical coordinate, positive upwards, with $z = 0$ at the mean sea surface, and z_0 is a reference depth. L_u and K_d were estimated in 3 m bins using a least squares minimization of (1) to all the observations in the bin that passed the tilt threshold criterion. This bin size was chosen based on results of simulations that mimicked the sampling characteristics of the observations (see also Zibordi et al. (2004)).

The uppermost bin spanned depths between about 4 and 1 m, centered at about 2.5 m. The attenuation coefficient, K_d , computed for that bin was used to propagate the near surface radiance upwards.

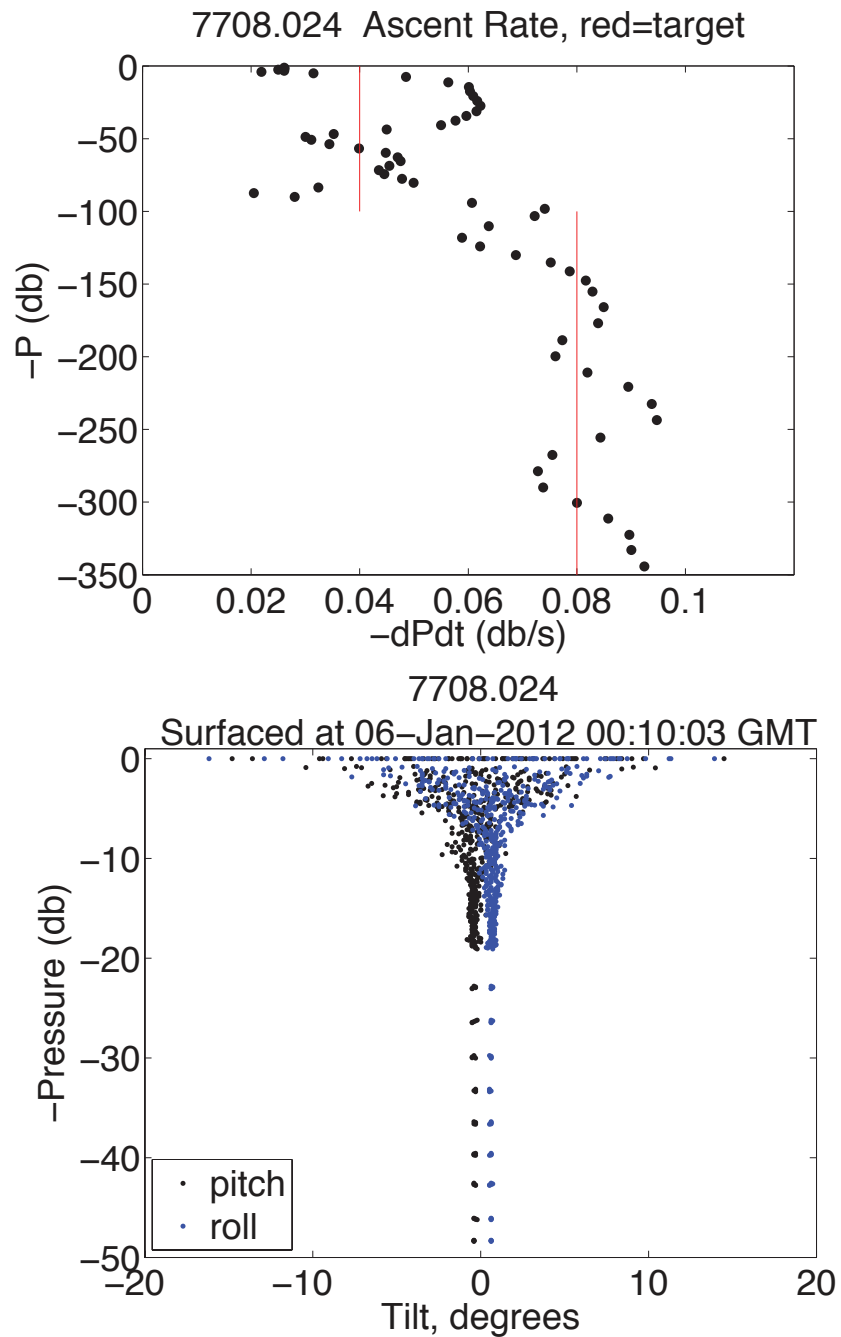


FIG. 2. Ascent rate and tilt of a float near the ocean surface for a profile near Hawaii in January, 2012. Upper panel: Ascent rate. The target rates were 8 cm/s at depth and 4 cm/s above 100 m. Bottom panel: Tilt of the float during burst sampling (below 20 m) and during continuous sampling (above 20 m). Waves are not felt significantly at depths below about 15 m.

Attenuation lengths, $1/K_d$, are usually an order of magnitude larger than the depth of the bin center, which minimizes the effect that errors in K_d have on estimates of $L_u(0-)$. After the radiance is extrapolated to immediately below the sea surface, it is propagated through the surface following Morel and Gentili (1996). Remote sensing reflectance is computed as

$$R_{rs} = \frac{L_w}{E_s}, \quad (2)$$

where L_w is upwelling radiance above the air-sea interface and E_s is downwelling irradiance above the air-sea interface.

The *in situ* estimates of R_{rs} are compared to satellite estimates from MODIS Aqua and VIIRS. Although full details of satellite processing are beyond the scope of this document, a few statements are necessary. Processing of satellite data was done following standard methods at the NASA GSFC Ocean Biology Processing Group. The floats surfaced around 1330 solar time to coincide with the average time of satellite overpass. Comparisons were made if the satellite and float measurements were made within one hour of each other. Satellite measurements were averaged from the 25 pixels surrounding the float. They were rejected based on criteria including the number of good pixels, variations between pixels, ratio of satellite-estimated E_s to a theoretical prediction, and both solar and satellite zenith angles.

d. Data Quality

Ensuring high quality of the *in situ* float data is essential for calibration and validation activities. We distinguish between two steps of quality control: rejection of individual samples within a profile, and rejection of an entire profile. Currently, individual samples are rejected based on tilt of the instrument. A tilt sensor is housed in the optics package that measures coincidentally with the radiometers; any time the tilt on either horizontal axis exceeds 5° , that data point is excluded from analysis. This often results in reductions of more than 50% of the observations at depths of a few meters.

Rejection of entire profiles is more difficult. The autonomous time dependent nature of these floats complicates quality assessment, especially related to determination of whether a day is cloudy or clear. Shipboard observations have humans present to examine cloudiness visually. Both shipboard and moored observations produce time series that can be examined for evidence of changing cloudiness. Because the floats measure at the surface for only 5-10 minutes, measuring the change of downwelling irradiance to determine changing cloudiness is of limited utility. Franz et al. (2007) compared their above-water measurements to a theoretical estimate of clear sky irradiance (Frouin et al. 1989) and rejected observations that differed from the prediction by more than a threshold amount.

For the data presented here, we use two quality control criteria based on float data to identify times when the observations are likely to be affected by clouds. Both examine the fit of Gershun's equation (1). By fitting this equation we estimate L_u and K_d for all four wavelengths in 3 m bins between 15 m and the surface. If any of these 20 estimates returns a negative value for K_d , the entire profile is rejected. Similarly, if any of the best fit estimates of L_u in the upper four bins is smaller than the estimate in the bin below, the entire profile is rejected.

In addition to these criteria, we have tested the use of an intensity criterion similar to Franz et al. (2007). Standard satellite ocean color quality control also uses this criterion, and we have found that data

rejected by this criterion in our *in situ* data are also often rejected by the satellite processing. The data presented here do not use this criterion. Other criteria examining the variability of the instantaneous observations of L_u and E_d are in development but are not sufficiently refined for use here.

Such additional criteria are shown to be necessary by profiles that pass criteria based on bin estimates of L_u and K_d but still appear to be affected by clouds (figure 4). In the north Atlantic profile on 11 May, 2012, a cloud clearly affects the observation of L_u but not sufficiently to cause the bin-averaged estimate of L_u to decrease upwards. We are currently developing and testing algorithms to reject profiles based on objective criteria associated with variability of L_u within bins. About 10% of the possible matchups passed quality control criteria for the satellites. Many of these were rejected by float quality control criteria.

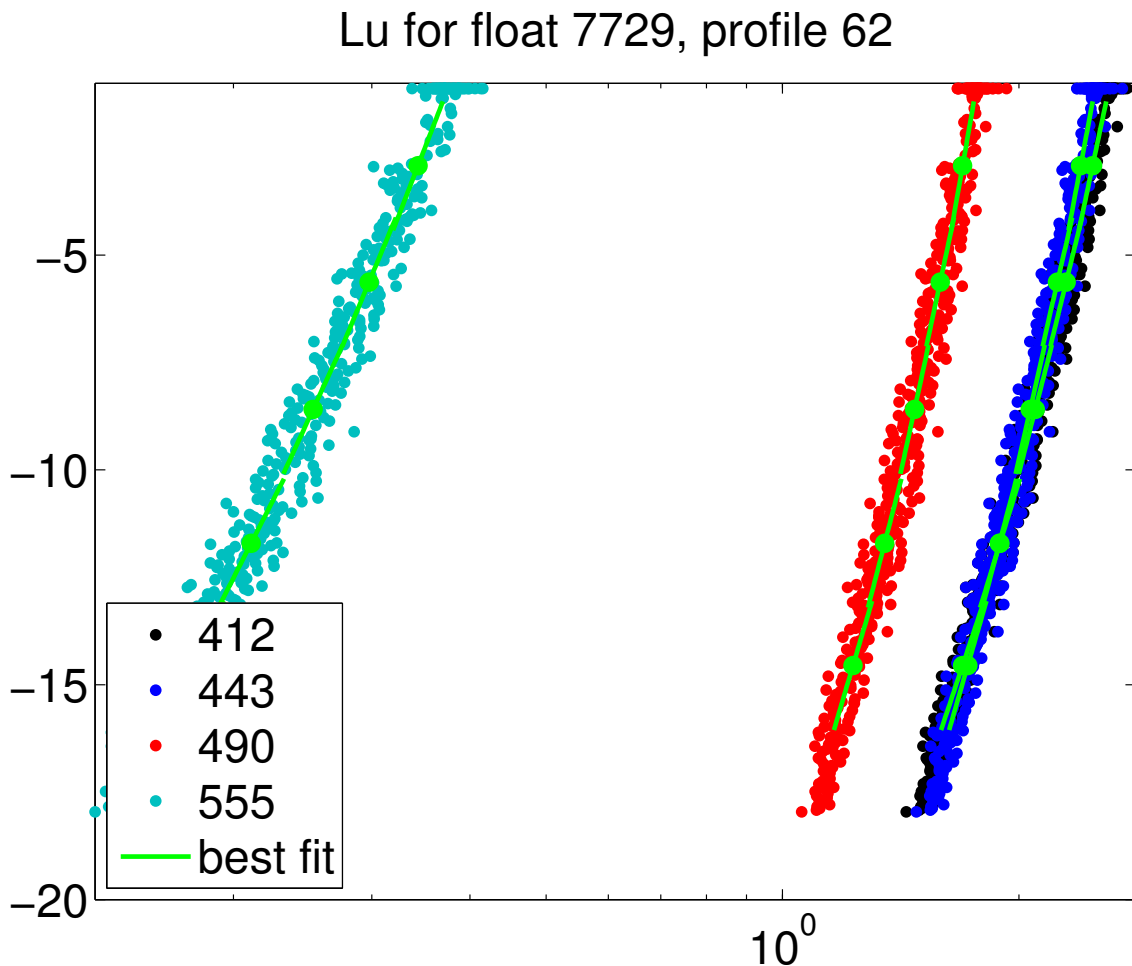


FIG. 3. Measurements of upwelling radiance, L_u , for all four wavelengths (412, 443, 490, and 555 nm) for a profile in the north Atlantic on 25 July, 2012. Superimposed on the profiles are the estimates of L_u in each bin center and the profile that is formed from that value and the best fit attenuation coefficient. The large number of values at 1.229 m demonstrated the measurements made while the float was at the sea surface.

Lu for float 7729, profile 17

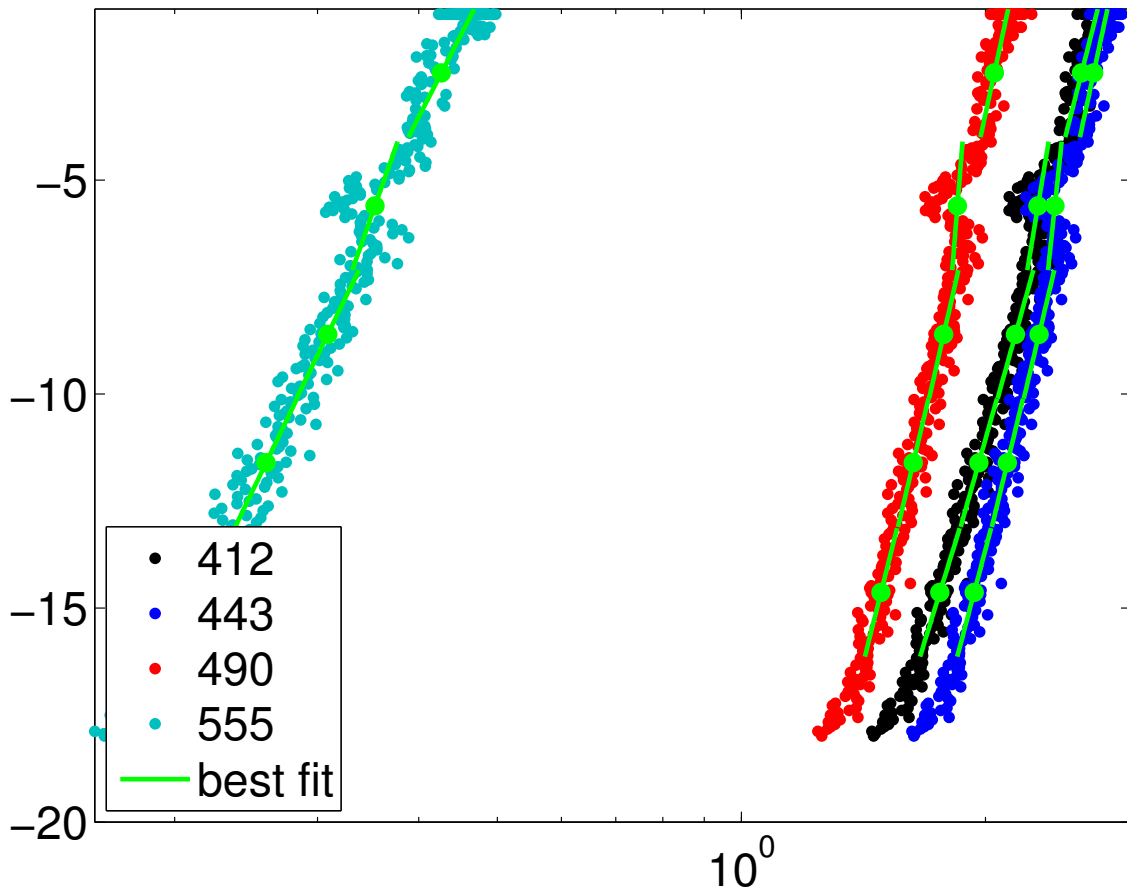


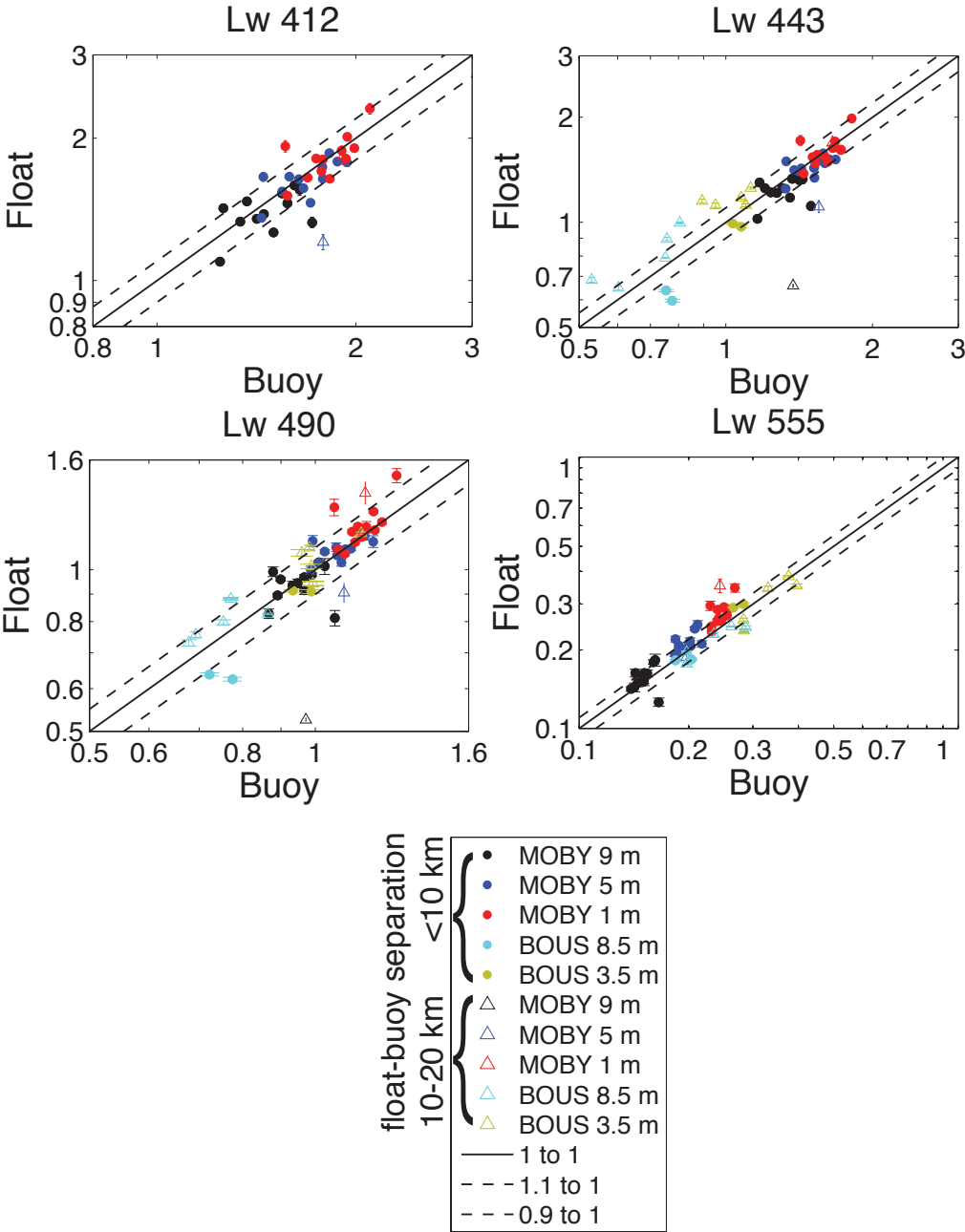
FIG. 4. Measurements of upwelling radiance, L_u , for a profile in the north Atlantic on 13 May, 2012. Superimposed on the profiles are the estimates of L_u in each bin center and the profile that is formed from that value and the best fit attenuation coefficient. The variability when the float is at 5 m depth is likely caused by passing clouds.

3. RESULTS

Roughly half the profiles were rejected because of at least one negative estimate of K_d . The remaining data are used to make three sets of comparisons: 1) in-water L_u measured by a float and a mooring when the floats were near the BOUSSOLE or MOBY moorings; 2) extrapolated L_w measured by a float and a mooring when the floats were near the BOUSSOLE or MOBY moorings; 3) R_{rs} measured by a float and a satellite.

The comparisons of float and moored estimates of L_u generally within 10%, and the agreement is better when the floats are within 10 km of the moorings (figure 5). For separations between 10 and 20 km the agreement begins to degrade, and comparisons were not made when the floats were more than 20 km from the moorings. Agreement is better for the 412, 443, and 490 nm wavelengths than it is for the 555 nm wavelength. Although we have fewer observations from BOUSSOLE than from MOBY, the quality of agreement appears initially to be similar at both sites. The 412 nm sensor at BOUSSOLE did not

function properly during the time of our deployments, limiting BOUSSOLE comparisons to only three wavelengths.



Units: $\mu\text{W}/\text{cm}^2/\text{nm}/\text{sr}$

FIG. 5. Comparison of upwelling radiance measured by a float and by the BOUSSOLE and MOBY optical buoys. Float observations are averaged into 1 m bins centered on the depth of the buoy radiometer. Dots represent observations within 10 km of the buoy. Triangles represent observations between 10 and 20 km from the buoy.

When upwelling radiance is extrapolated up through the sea surface, we have many fewer observations that met quality control standards for both the floats and buoys. Agreement remains within 10% for most samples, however (figure 6). As with the L_u comparisons, agreement at 555 nm is slightly worse than agreement at other wavelengths.

Agreement between float observations and satellite observations is not as good as that between float observations and mooring observations (figure 7). The float wavelengths of 412, 443, 490, and 555 nm are compared to MODIS-Aqua wavelengths of 412, 443, 488, and 547 nm and to VIIRS wavelengths of

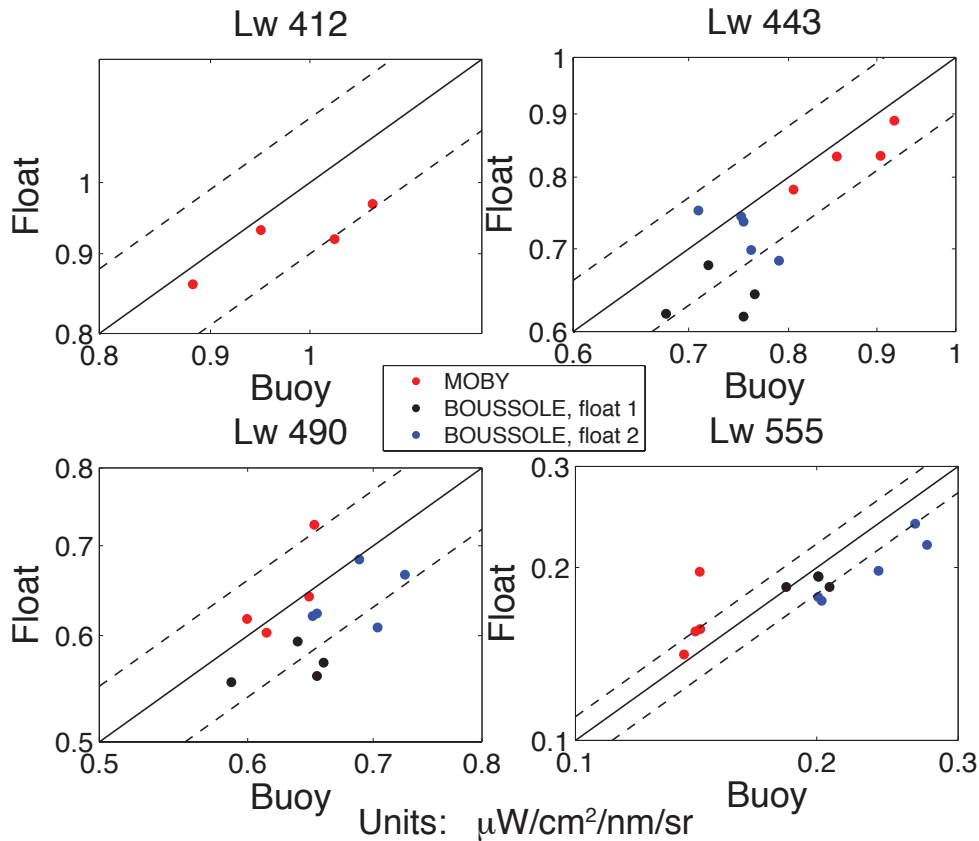


FIG. 6. Comparison of water leaving radiance measured by a float and by the BOUSSOLE and MOBY optical buoys for each wavelength of the float.

410, 443, 486, and 551 nm. For all wavelengths except 555 nm, mismatches are usually 20% or smaller. For 555 nm mismatches are larger. In addition, slight bias is evident in comparisons between MODIS-Aqua and the floats at 490 and 555 nm. Unfortunately, quality control procedures for VIIRS left matchups only with the float near Hawaii so the comparisons with VIIRS are limited. VIIRS has not yet undergone a vicarious calibration process, but comparisons between float and VIIRS observations are not substantially worse than comparisons between float and Aqua measurements, suggesting a reasonable initial calibration of the VIIRS sensors.

4. DISCUSSION

This study has not yet quantified uncertainties in observations or the effects of biofouling on observation quality. The major dynamic sources of uncertainty in the radiometric measurements are wave focusing of light near the surface and uncertainties in sensor depth during ascent. Of the floats that we have

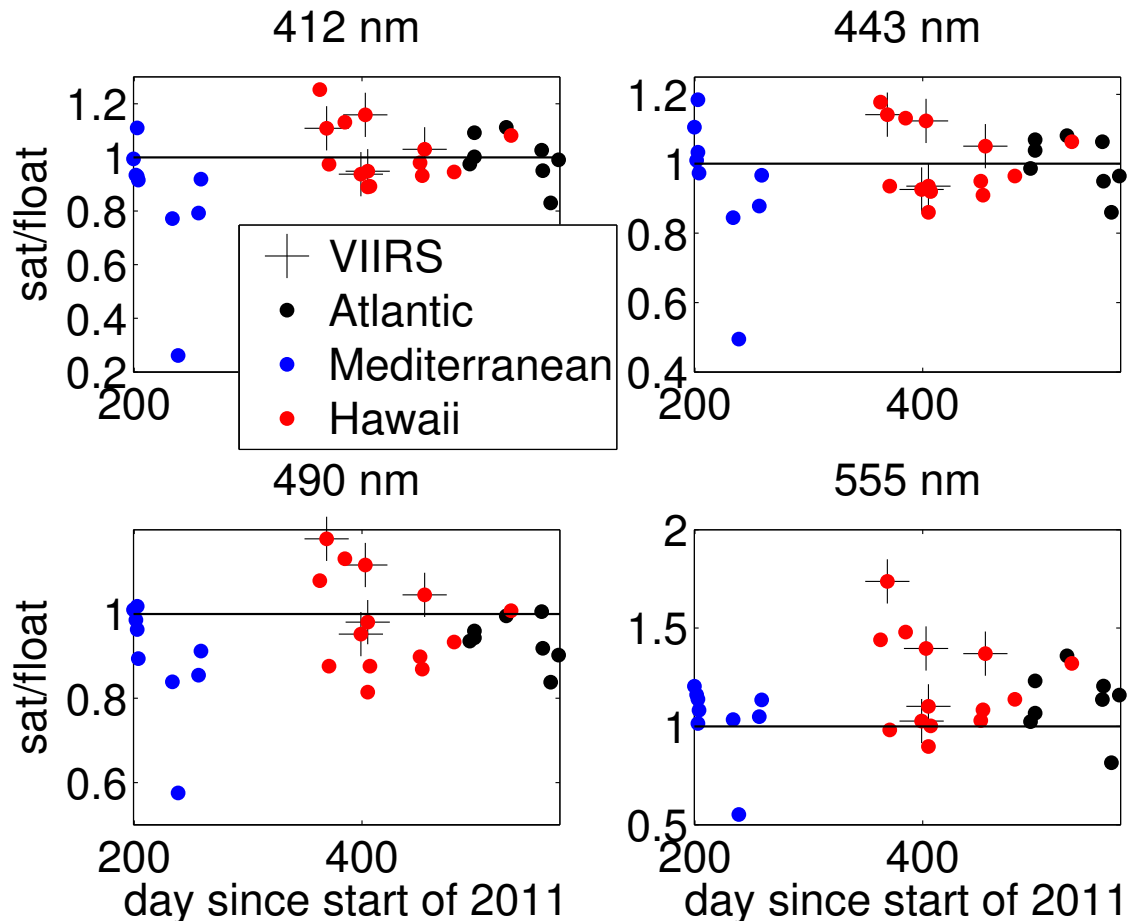


FIG. 7. Ratios of R_{rs} measured by MODIS-Aqua or VIIRS to R_{rs} measured by the floats. Each wavelength is shown in a different panel and the colors show the locations of the float deployments. Note the different axis scales in each panel. Variability is larger than that seen by Franz et al. (2007) and Bailey et al. (2008) in comparisons of *in situ* and satellite observations.

deployed, the high frequency (0.5 Hz) pressure measurements have been implemented only on the floats in the north Atlantic, not those that were deployed in the Mediterranean Sea or near Hawaii. In the older pairs of floats the ascent rate varies near the surface, and pressure measurements are made only about once per minute. This leads to an opportunity for substantial uncertainty in the pressure estimates for each radiometer sample (which are measured at about 1Hz). Fortunately, these uncertainties are only felt through their effects on the attenuation coefficients which are used to propagate L_u to the surface. For cases in which the attenuation length scale is 20 times larger than the measurement depth of the surface sample (as is the case in these measurements), a 10% error in K_d leads to only a 1% error in L_w .

Our fitting of (1) to the observed radiances is similar to the technique developed by Zaneveld et al. (2001) to smooth out the effects of wave focusing of solar radiation. The chief requirement for this to be effective is that the ascent rate must be small compared to the space- and time- scales of wave fluctuations (see Zibordi et al. (2009) for more discussion). The ascent rate of 4cm/s was chosen in an attempt to satisfy this criterion within the range of capabilities of the float.

The good agreement of the float with the buoy observations suggests that floats may be a useful supplement to buoys for calibration and validation of satellite observations. In addition, further refinement of rejection criteria for the float data may lead to improved agreement of float observations to satellite observations. More float deployments and a larger number of comparisons are necessary to develop robust quantitative comparisons of float data to both buoy and satellite data.

5. ACKNOWLEDGEMENTS

We Thank NASA for their support of this project and the MOBY group for assistance with float deployment and data. Rebecca Conneely was a great help in determining optimal bin sizes for parameter estimations.

REFERENCES

- Antoine, D., P. Guevel, J.-F. Diesté, G. Bécu, F. Louis, A. J. Scott, and P. Bardey, 2008: The “BOUSSOLE” buoy—a new transparent-to-swell taut mooring dedicated to marine optics: Design, tests, and performance at sea. *Journal of Atmospheric and Oceanic Technology*, **25**, 968–989.
- Bailey, S. W., S. B. Hooker, D. Antoine, B. A. Franz, and P. J. Werdell, 2008: Sources and assumptions for the vicarious calibration of ocean color satellite observations. *Applied Optics*, **47** (12), 2035–2045.
- Clark, D. K., et al., 2003: *MOBY, a radiometric buoy for performance monitoring and vicarious calibration of satellite ocean color sensors: measurement and data analysis protocols*. NASA Tech. Memo. 2004-211621, NASA, Goddard Space Flight Center, Greenbelt, MD (2003).
- Franz, B. A., S. W. Bailey, P. J. Werdell, and C. R. McClain, 2007: Sensor-independent approach to the vicarious calibration of satellite ocean color radiometry. *Applied Optics*, **46** (22), 5068–5082.
- Frouin, R., D. W. Lingner, C. Gautier, K. S. Baker, and R. C. Smith, 1989: A simple analytical formula to compute clear sky total and photosynthetically available solar irradiance at the ocean surface. *Journal of Geophysical Research*, **94** (C7), 9731–9742.
- Hooker, S., C. McClain, and A. Mannino, 2007: *NASA Strategic Planning Document: A comprehensive plan for the long-term calibration and validation of oceanic biogeochemical satellite data*. NASA Tech. Rep. Series: NASA/SP-2007-214152.
- Morel, A. and B. Gentili, 1996: Diffuse reflectance of oceanic waters. III. implication of bidirectionality for the remote-sensing problem. *Applied Optics*, **35** (24), 4850–4862.
- Voss, K. J., et al., 2010: An example crossover experiment for testing new vicarious calibration techniques for satellite ocean color radiometry. *Journal of Atmospheric and Oceanic Technology*, **27**, 1747–1759.
- Werdell, P. J., S. W. Bailey, B. A. Franz, A. Morél, and C. R. McClain, 2007: On-orbit vicarious calibration of ocean color sensors using an ocean surface reflectance model. *Applied Optics*, **46** (23), 5649–5666.
- Zaneveld, J. R. V., E. Boss, and A. Barnard, 2001: Influence of surface waves on measured and modeled irradiance profiles. *Applied Optics*, **40** (9), 1442–1449.
- Zibordi, G., J.-F. Berthon, and D. Dalimonte, 2009: An evaluation of radiometric products from fixed-depth and continuous in-water profile data from moderately complex waters. *Journal of Atmospheric and Oceanic Technology*, **26**, 91–106.
- Zibordi, G., D. Dalimonte, and J.-F. Berthon, 2004: An evaluation of depth resolution requirements for optical profiling in coastal waters. *Journal of Atmospheric and Oceanic Technology*, **21**, 1059–1073.